Metrology for Characterizing Scratch Resistance Of Polymer Coatings

Li-Piin Sung and Peter L. Drzal—*National Institute of Standards and Technology**
Mark R. VanLandingham—*U.S. Army Research Laboratory*[†]
Tsun Yen Wu and Shuo-Hung Chang—*National Taiwan University***

Current methods for scratch resistance assessment are often based on "relative but not quantitative" types of measurements, such as visual inspection, gloss changes, and changes in gray scale level or lightness. Most results are used for qualitative assessment purposes, which result in the lack of a repeatable and reliable standardized test method for the polymer materials community. To implement a scientifically based standardized test method for quantifying scratch resistance, it is vital to understand the relationships between material mechanical properties, morphology, and appearance (optical properties) of surface and subsurface deformation. In this article, preliminary results from a scratch testing protocol to identify the "onset" of plastic deformation in poly(methyl methacrylate) and poly(propylene) commercial samples are presented. Recent advances in optical scattering measurements to identify the onset of plastic deformation by analyzing specular and off-specular intensities are also presented.

Keywords: Hardness, scratch resistance, surface analysis, light scattering, gloss measurement, laser scanning confocal microscopy, appearance, durability, mechanical properties

S cratch resistance is a desirable characteristic and is widely used as a key critical performance property in both industry and research laboratories for evaluating the durability of polymer coatings and plastic products. Various instruments for assessing scratch resistance and test methods[1-6] have been developed to quantify and rank scratch resistance with respect to the imposed scratch conditions. Many researchers have tried to relate mechanical properties, such as tensile strength,[7,8] for example, to scratch resistance or to correlate scratch resistance to toughness through the analysis of fracture energy.[9] As a result, current scratch test methods are highly dependent on the test or system used, and the test conditions, which include parameters such as tip material/geometry, force/depth range, and velocity/length. Consequently, scratch test results can vary widely depending on the materials and testing environment, making it difficult to compare the results of scratch tests between laboratories.

The wide variety of scratch methods and instrumentation present many challenges in the standardization of scratch protocols. Equally difficult to standardize is the assessment and measurement of scratch resistance. Scratch resistance is commonly measured by assessing appearance changes brought about by scratch damage. Scratch damage can range from plastic grooving in a ductile material, to cracking and chipping in a brittle material. Scratch resistance assessment is often based on "relative but not objective" types of measurements, such as visual inspection, gloss changes, and changes in gray scale level or lightness. These assessments are only qualitative. More quantitative approaches, such as those described in a recent study by Rangarajan et al.,[10] used optical imaging techniques to quantify the visibility of a scratch on a glossy polymer surface. These results emphasized the importance of optical contrast between the damage area and its surroundings. The total optical contrast is a combination of scratch size and the contrast in specular and off-specular scattering. A good correlation between the total optical contrast and visibility of a scratch was proposed by an industrial appearance perception study.[11] However, this study does not report on the relationship between the appearance assessment of scratch and the associated material mechanical response.

In order to properly understand the scratch resistance of materials, both the tip-sample interaction that causes the scratch damage and the resulting change in optical perception must be studied. To address these issues, researchers from NIST and industry (through a National

---

Institute of Standards and Technology (NIST)/industrial Polymer Interphase Consortium (PIC)[12]) have proposed a methodology to quantitatively relate surface deformation (scratch morphology) to appearance attributes in order to quantitatively evaluate the scratch resistance of polymer coatings and plastics. In this article, we discuss the proposed scratch test methodology, including preliminary optical scattering measurements of scratch profiles and their relationship to damage morphology.

EXPERIMENTAL*

Materials

Materials used in this study included poly(methyl methacrylate) (PMMA), and high crystalline poly(propylene) (PP). PMMA samples approximately 3.8 mm thick were provided directly from a commercial source. Injection-molded plaques of PP, approximately 3 mm thick, were provided by Dow Chemical. For the optical scattering studies, black-pigmented PP samples were selected to reduce subsurface scattering so that the scattering due to scratch damage near the surface could be collected. All samples were used as received with no further annealing or modifications. The representative indentation modulus of PMMA and PP are (5.11 ± 0.08) GPa and (1.33 ± 0.07) GPa, respectively.[13] These values were obtained using an MTS DCM nanoindenter and evaluated at an indentation depth of 1 μm. The error bars represent one standard deviation (k=1) from 10 individual indentations.

Certain instruments or materials are identified in this article in order to adequately specify experimental details. In no case does it imply endorsement by NIST or imply that it is necessarily the best product for the experimental procedure.

Scratch Testing

Scratch testing was performed using the MTS Nanoindenter XP equipped with lateral force measurement capability, and has been described elsewhere.[13] All scratches were generated using 45° semi-apical angle diamond cone indenters with a tip radius of 1 μm or 10 μm. Scratches were generated by either progressive force or constant force scratch methods. A progressive force scratch test linearly increases the applied force over the length of the scratch. Constant force scratch tests maintain a constant force over the length of the scratch. The instrument also measures the scratch and residual depths, friction coefficient, and residual roughness during scratch testing. The estimated uncertainties of these quantities are one standard deviation from the mean determined from at least three scratch tests.

Scratch Morphology Characterization

A Zeiss model LSM510 reflection laser scanning confocal microscope (LSCM) was employed to characterize the surface morphology of scratches (topographic profile, surface roughness, and width). A detailed description of LSCM measurements can be found elsewhere.[14,15] The laser wavelength used in this study was 543 nm. *Figure* 1 shows examples of scratch profiles produced by (a) progressive force and (b) constant force scratch test methods. The scratch width was defined as the peak-to-peak distance and is indicated in *Figure* 1b. LSCM images are two-dimensional (2D) intensity projections resulting from a series of overlapping optical slices (a stack of z-scan images) with a z-step of 0.1 μm. The 2D intensity projection images are effectively the sum of all the light scattered by different layers of the coating, limited by the maximum depth of light penetration. The pixel intensity level represents the total amount of back-scattered light. The estimated uncertainties of scratch width measurements were one standard deviation from the mean determined from 10 different locations on each scratch profile.

Optical Scattering Measurements of Scratches

Optical scattering measurements using a newly constructed light scattering instrument were conducted at various incident angles in the specular, off-specular, and out-of-plane scattering configurations on a variety of scratch profiles. The new instrument, located in the NIST Building and Fire Research Laboratory, consists of a laser light source, a five-axis goniometric sample stage, and a 2D detector mounted in a concentric ring around the sample stage (see *Figure* 2a). The incident laser wavelength was 633 nm, and the beam was polarized and focused on the sample with a diameter of 1 mm. The sample rotation stage and the detector ring posi-
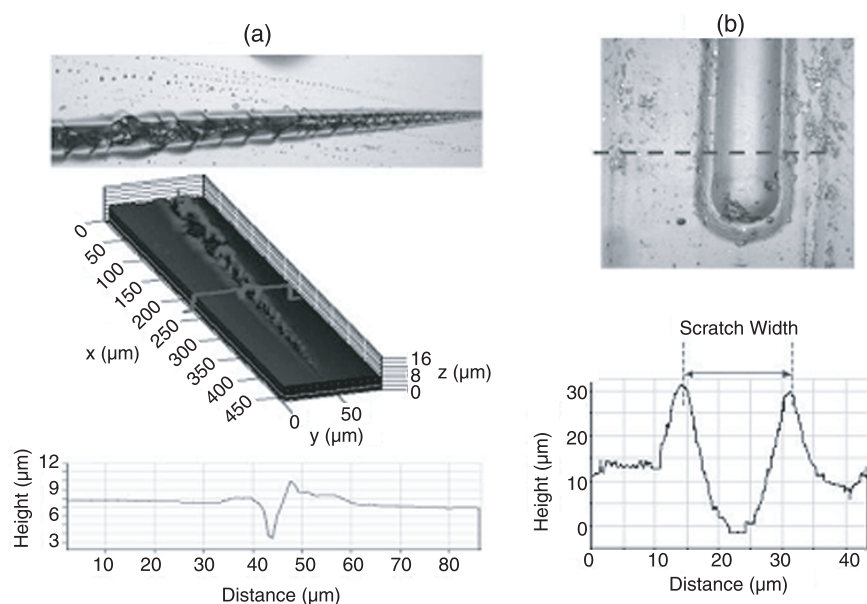

Figure 1—LSCM images of (a) scratch produced by a progressive force scratch method: 2D intensity projection (top) and 3D topological presentation with line profile (bottom); (b) scratch produced by a constant force scratch method: 2D intensity projection (top) and height profile (bottom).

tion determine the incident angle of the beam on the sample and the viewing angle of the detector. *Figure* 2b presents the optical geometry, where θ_i and θ_s are the incident and scattering angles measured with respect to the normal of the sample. The sign convention is such that $\theta_s = \theta_i$ indicates the specular reflection angle. A detailed description of the instrument will be reported elsewhere.[16] In this article, we present the results in terms of the 2D angular distribution of light scattered from a scratch surface at an incident angle of 45°. The scattering signal from scratch is compared to the background signal from the coating surface, and the ratio of these two is used to evaluate the visibility of the scratch. A brief visual inspection is correlated with the optical measurements.
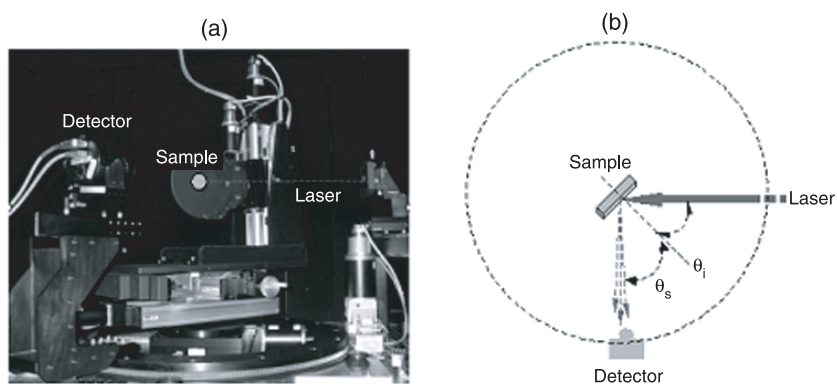

Figure 2—(a) Photo of the incident laser beam, goniometric sample stage, and a 2D detector; (b) top view of the layout and optical geometry for the incident, θ_i, and scattering, θ_s, angles, respectively.

RESULTS AND DISCUSSION

Preliminary Measurement Protocol for Scratch Test

After an intensive study of scratch testing using various tip geometries, scratch loads, and scratch velocities, we have developed a measurement protocol for scratch testing using the MTS Nanoindenter XP instrumentation. This measurement protocol is designated as the Polymer Interface Consortium Scratch Test Protocol (PICSTP). This preliminary measurement protocol is described briefly as follows: (1) A series of progressive force scratch tests imparts a number of scratches with a range of severity in deformation. (2) LSCM (or a high-resolution optical microscopy) is used to characterize the resulting surface deformation and identify the "onset" of plastic deformation. (3) Constant force scratch tests are conducted over a range of forces in the vicinity of the onset of plastic deformation. (4) LSCM is used to analyze the constant force scratches to identify more accurately the force that corresponded to the onset of plastic deformation. (5) Important scratch features such as scratch width, yield coefficient of friction, scratch depth, and residual depth at the onset of plastic deformation are identified from LSCM and scratch data. (6) Scratch test results are correlated with visual inspection and optical scattering measurements.

Scratch Test for PMMA System

Figure 3 demonstrates the application of the PICSTP on the PMMA sample. *Figure* 3a is an image that corresponds to the scratch profile produced by a progressive force test using the 1-μm cone. The scratch load ranged from 0 mN to 30 mN over a total scratch length of 500 μm using a
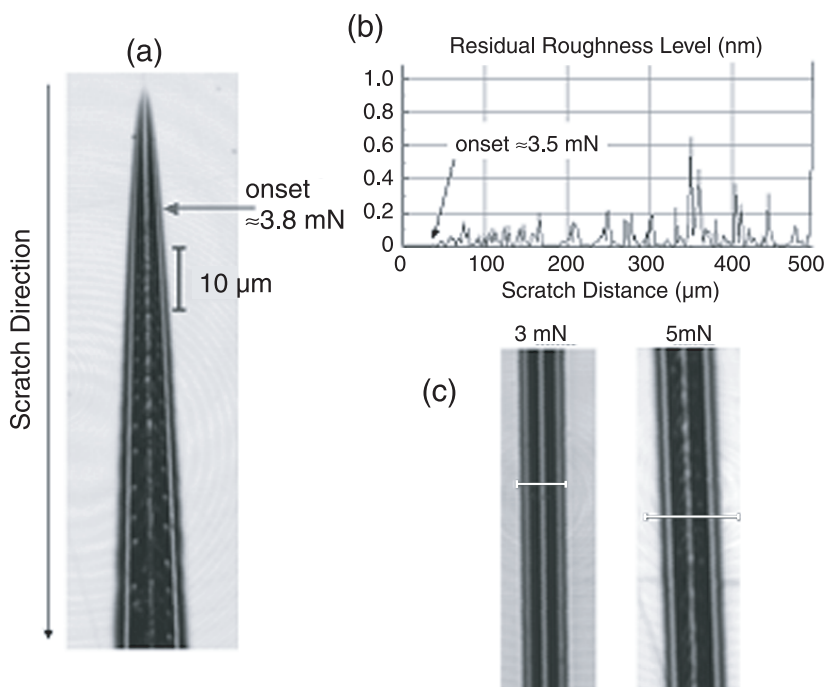

Figure 3—(a) LSCM image of a scratch (on PMMA) produced by a progressive force test. The onset is indicated at the point where plastic cracking occurred. (b) The residual roughness level obtained from the progressive force test in (a) and the onset defined as a significant increase in the residual roughness level. (c) Two scratches produced by constant force tests below (3 mN) and above (5 mN) the onset load.

scratch velocity of 1 μm/sec. Plastic deformation in the form of a concave deformation pattern was observed along the scratch direction. This type of pattern is typical of materials that have undergone "brittle" failure.[17] The onset of this plastic deformation was determined by two different methods. The first method used LSCM to identify the start of the deformation pattern, as shown in *Figure* 3a. The second method, shown in *Figure* 3b, determined the onset at the point where the residual roughness level became significant. Both methods measured similar onset points for the PMMA sample. Constant force tests (*Figure* 3c) at force values above and below the "critical load" were then conducted to define the onset point more precisely. The critical load was determined to be (3.8 ± 0.2) mN for the PMMA sample from these constant force tests.
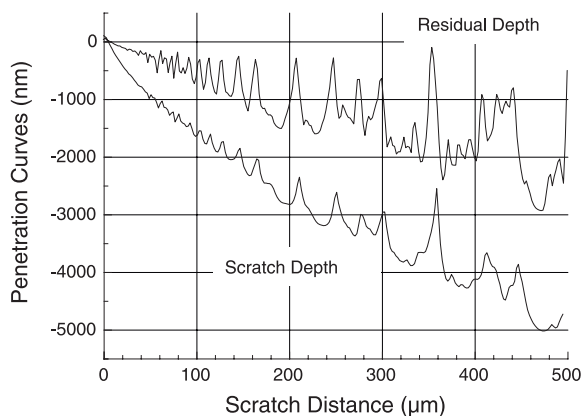
Figure 4—Plot of penetration data recorded by the indentation instrument during the progressive force scratch tests described in *Figure* 3 for PMMA. The lower curve represents the penetration depth during the scratch, whereas the upper curve represents the unrecovered depth (residual depth) remaining just after scratching. The estimated uncertainty in one standard deviation (k=1) in the data is about 3%.

Additional measurements of scratch response unique to each type of material were also collected. *Figure* 4 shows the scratch penetration data generated by the instrument during progressive force scratch tests. The perturbations in the penetration profiles are the result of "stick-slip" behavior corresponding to the formation of the deformation pattern. The corresponding residual depth and scratch width were estimated to be (500 ± 20) nm and (6 ± 1) µm, respectively. At the onset point, the recovery rate (elasticity) was determined to be 56%.

The relationship between the scratch velocity and the surface damage (depth, width, and the onset) was also in-

vestigated. *Figure* 5a shows the scratch damage obtained with the conical indenter with 4 mN of force at different velocities with PMMA. The measured scratch width was approximately 30% wider at 1 µm/sec than at 100 µm/sec. The velocity dependence on scratch deformation demonstrates one way in which polymer viscoelasticity affects scratch resistance. In this case, the material acts stiffer at higher scratch velocities and results in less plastic deformation. Similar trends were observed between scratch and residual depths and scratch velocities for constant force tests. *Figure* 5b and 5c show the semilog plot of scratch/residual depth and scratch width as a function of scratch velocity, respectively. The residual depth decreased from around 570 nm at 1 µm/sec to around 400 nm at 100 µm/sec, and the recovery rate (elasticity) changed from 56% at 1 µm/sec to 63% at 100 µm/sec for a scratch force of 4 mN, respectively. In both plots, a linear relationship (inversely correlated) was observed in the semilog plot, i.e., depth (or width) ≈ log (velocity).

Scratch Test for the PP System

The PICSTP methodology was also applied to the PP samples using the same 1-µm radius conical indenter at a velocity of 1 µm/sec and is summarized in *Figure* 6. Noticeably, the scratch morphology of PP system was quite different from the PMMA. In this case, a convex deformation pattern was observed. This scratch pattern is typical for tough materials like polyolefins. When compared to the PMMA, the scratch damage appeared at lower values of force and resulted in more severe plastic deformation. The "onset" obtained from the LSCM image (*Figure* 6a) and the residual roughness level data (*Figure* 6b) of a progressive force scratch test (0 mN to 30 mN) were estimated at 1.2 mN and 1.8 mN, respectively. The constant force scratch tests conducted at forces below the critical load, shown in *Figure* 6c, however, continued to generate plastic deformation. The low forces required for scratch deformation in the PP made the isolation of the critical load difficult from both the residual roughness and the LSCM image. A larger radius cone was then used in an attempt to better resolve the forces at which plastic deformation occurred. *Figure* 7 shows the scratch test results for the same PP sample with a 10-µm radius cone. Although the force resolution was better with this indenter, the onset of plastic deformation remained difficult to isolate from a progressive scratch. Onset values determined from LSCM images or the residual roughness level were restricted by instrumental limitations and are shown in *Figure* 7a and 7b. A series of constant force scratches using the 10-µm cone, shown in *Figure* 7c, provided better identification of the onset near 4 mN.
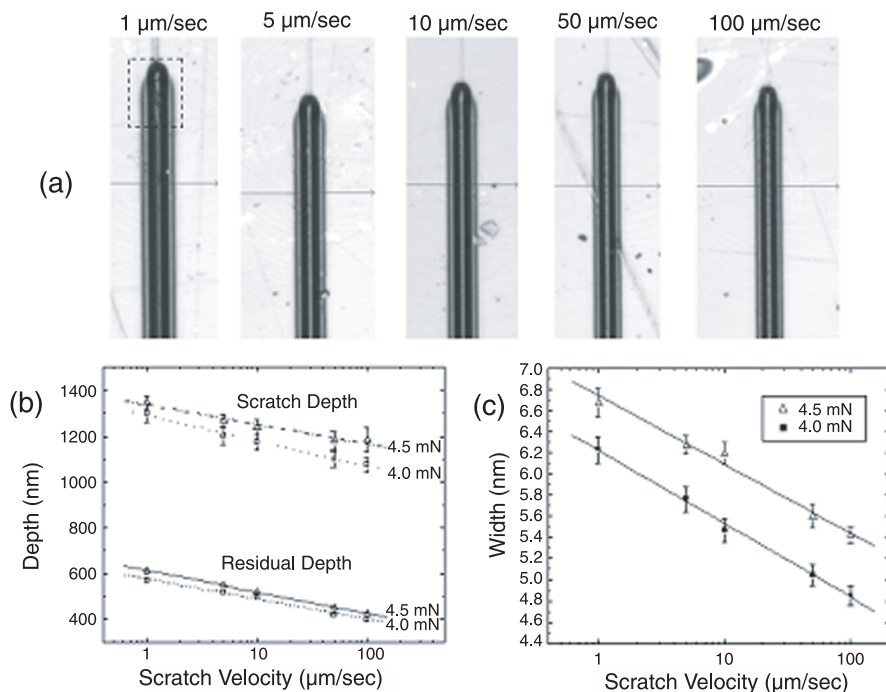

Figure 5—(a) Scratch profiles including the scratch width of PMMA samples at 4 mN for five different scratch velocities. Semilog plots of (b) scratch and residual depths and (c) scratch width vs. scratch speed for two different scratch forces. The lines are the linear fit to data in the semilog plots. The error bars represent an estimated standard deviation (k=1).

A comparison of the critical loads determined with the two different tips demonstrated the advantage of the constant force scratch test method to better identify the elastic-plastic transition. The comparison also emphasized that the critical load varies with tip shape. An alternative parameter such as "critical strain" or "critical stress" would be a more appropriate representation of the critical parameter and has been suggested by other researchers.[18] Conversion of load and displacement data to average stress and strain accounting for tip shape calibration[19,20] are the focus of continuing research efforts.

Additional information about the elastic recovery of the PP was also determined. Measurements of the applied deformation and the residual damage from both progressive and constant force tests are shown in *Figure 8*. The recovery rate at low scratch loads (less than 3 mN) was almost 100%. The recovery dropped to 86% at 4 mN and further to 48% at 30 mN.

Optical Scattering Characterization Of a Single Scratch

During the process of scratch deformation, the scratching probe generated dynamic and complex stress and strain that interacted with the polymeric coating. The mechanical properties of the coating determine what combination of elastic and plastic deformation the polymeric coating will utilize to dissipate the applied energy. The contribution of different deformation mechanisms determines the overall shape, magnitude, and characteristics of the resulting scratch. The point at which the scratch becomes visible and spoils the appearance is the greatest concern to coating manufacturers. These scratches are often called light scratches and differ from severe scratches that are generated from catastrophic plastic deformation. Specular gloss or gray scale level measurements can be used to assess the appearance changes due to heavy scratch damages, but these types of measurements are often not sensitive enough to detect light scratches. Appearance perception studies[11] showed that people were more perceptive to light scratches by varying the viewing angles. It is important, therefore, to implement a higher resolution technique to distinguish the "signal" of a light scratch from that of unscratched surface without relying on human

perception. With a threshold of visibility established, polymeric materials will then be able to be evaluated in the context of how much energy was required to generate a perceptible scratch. The remainder of this article concentrates on our progress toward optically determining the scratch perception threshold.
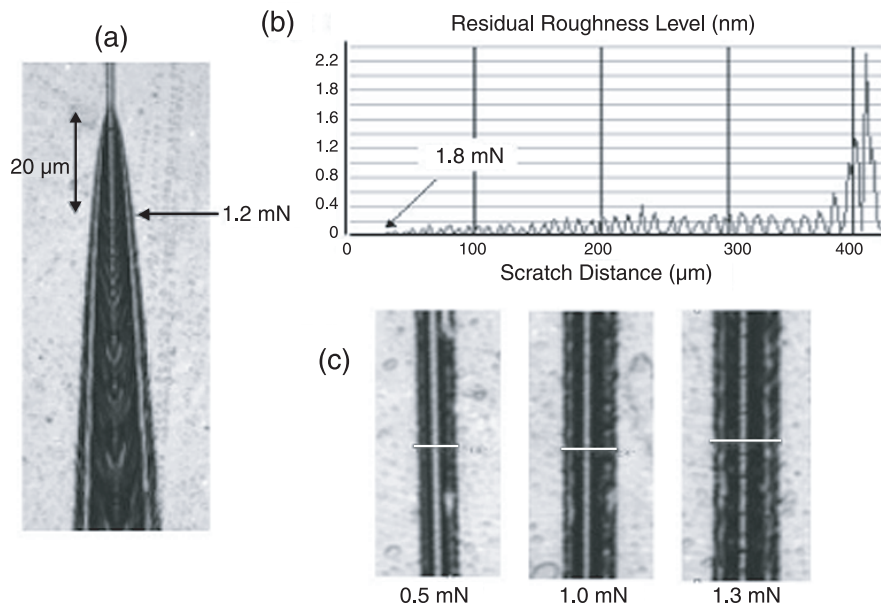

Figure 6—(a) LSCM image of a scratch (on PP) produced by a progressive force test using 1 μm indenter tip. (b) The residual roughness level corresponding to the scratch progressive force test in (a) as a function of scratch distance. (c) Three scratches produced by constant force tests below and near the onset load.
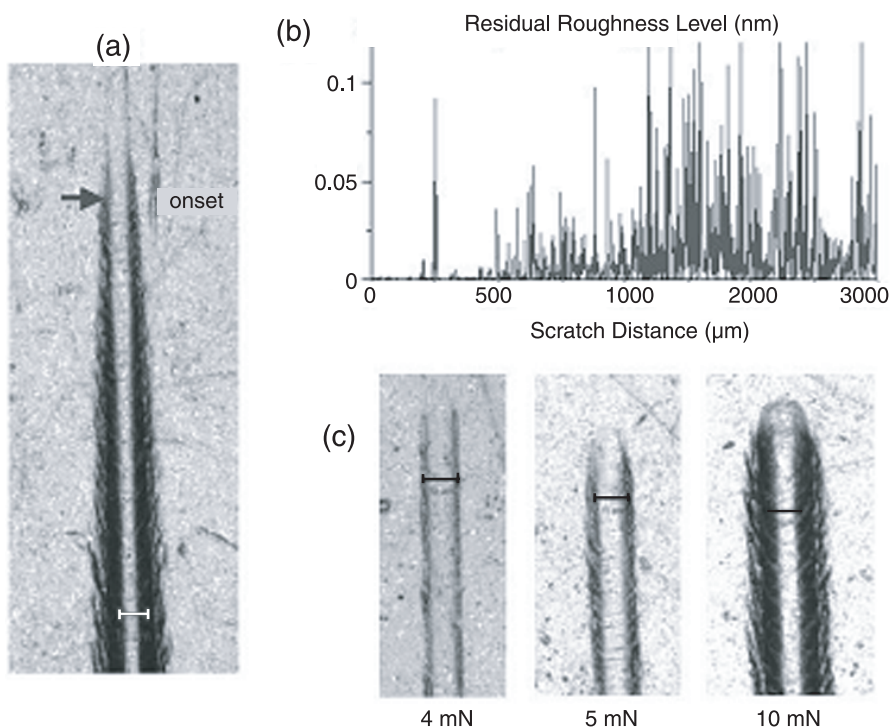

Figure 7—(a) LSCM image of a scratch (on PP) produced by a progressive force test using 10 μm indenter tip. (b) The residual roughness level corresponding to the scratch progressive force test in (a) as a function of scratch distance. (c) Three scratches produced by constant force tests: 4 mN, 5 mN, and 10 mN.
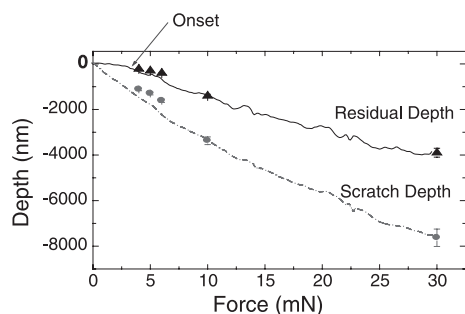
Figure 8—Scratch and residual depths as a function scratch force for a PP sample and a 10 μm conical indenter. The lines are data produced from the progressive force test and the symbols are data generated by constant force tests. Scratch velocity is 1 μm/sec.

Using the newly constructed light scattering instrument at NIST, optical scattering measurements on a single scratch at various scattering geometries collecting both the specular and nonspecular intensities were conducted. *Figure* 9 shows optical scattering measurements of the unscratched surface (*ns*) and two 3-mm single scratches (*s2* and *s3*) of the PP sample and the corresponding scratch morphology measured by LSCM. Scratch *s2* was made with a scratch force of 1 mN less than the onset load and scratch *s3* was made at a scratch force of 2 mN greater than the onset load. The laser light with an incident angle of 45° was focused on the middle of the scratch and the orientation of scratch with respect to the laser indicated in *Figure* 9. By visual inspection, scratch *s2* was hardly visible, while scratch *s3* was clearly noticeable. The 20° specular gloss measurements at all three surfaces from a handheld

commercial glossmeter (Minolta, Multi-Gloss model 268) were indistinguishable: all values were between 56.4 ± 1.0 within measurement uncertainty.

The scattering profiles (*Figure* 9a and 9b) from the unscratched surface and two scratches are distinguishable. *Table* 1 lists the calculated scattered intensity for specular gloss intensity, and the total intensities from scattering profiles (a) and (b). The specular gloss intensity was obtained by integrating the scattered intensity within the angular range of 45° ± 0.9°. Similar to the results from the commercial glossmeter, there was little difference in specular gloss intensity for three surfaces. In order to distinguish the visibility of two scratches, the nonspecular scattered intensity must be measured. Scratch parameters, such as size, shape, depth of the scratch, pile-up, and roughness of unscratched surface, have a strong impact on the scattered intensity distribution. The total scattered intensities listed in *Table* 1 of scratch *s3* are greater than those values of *ns* and *s2* for both near-specular ($\theta_s = 43°$, $\alpha = 0.5°$) and off-specular ($\theta_s = 40°$, $\alpha = 0.5°$) configurations. Here, θ_s and α are the scattering angle (as defined in *Figure* 2) and the out-of-plane scattering angle, respectively. This preliminary result indicated that the onset of a visible scratch can be determined from optical scattering experiments. Current research has been dedicated to replicating these measurements on scratches with different features, such as surface roughness, subsurface microstructure, and color. These features will affect the scratch visibility. Future work will include reporting the "visibility" of the scratch by comparing the scratch signal to the background signal from the unscratched surface.
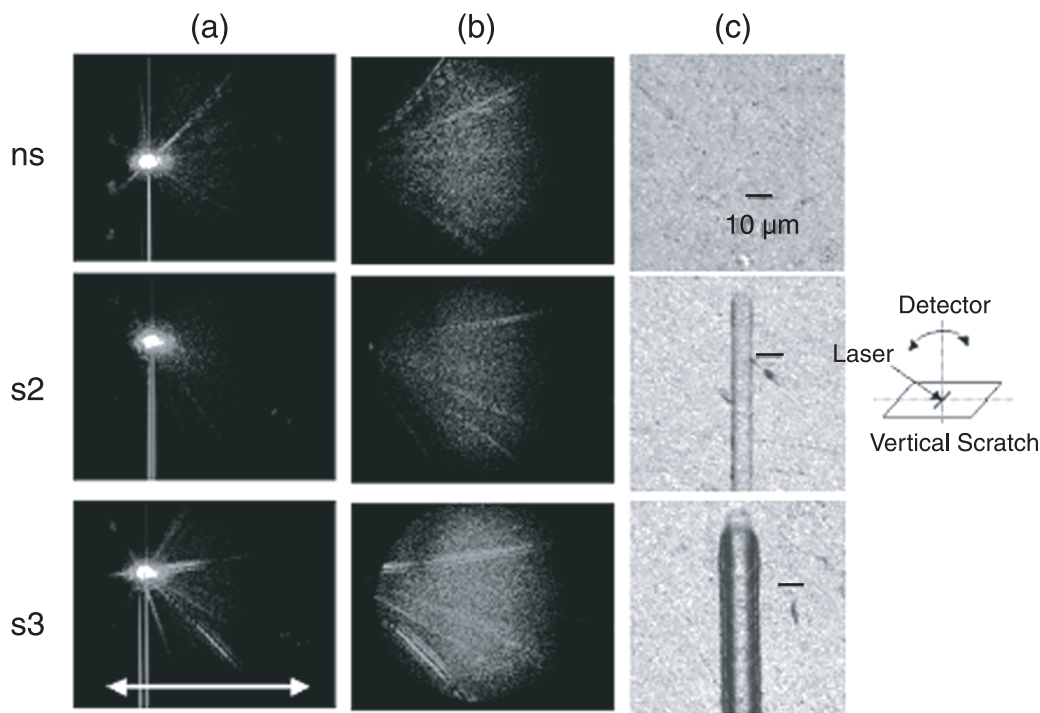

Figure 9—Scattered intensity patterns of the surface (*ns*) and two single scratches (*s2, s3*) of a PP sample from (a) at ($\theta_s = 43°$, $\alpha = 0.5°$) configuration and (b) at ($\theta_s = 40°$, $\alpha = 0.5°$) configuration. The corresponding LSCM images of that surface with and without scratch are also shown in the third column. The size scale (↔) covers an angular range of 7°. Here, θ_s and α are the scattering angle and the out-of-plane scattering angle, respectively.

Table 1—Total Scattered Intensity from Unscratched Surface (*ns*), Two Single Scratches (*s2*, *s3*) at (a) and (b) Scattering Configurations from *Figure* 9

Scattering Location	Gloss Intensity[a] (Specular Angle ± 0.9°) (x 10^6 counts)	Total Intensity from (a) (x 10^6 counts)	Total Intensity from (b) (x 10^6 counts)
ns	2.20 ± 0.06	6.91 ± 0.06	0.15 ± 0.04
s2	2.16 ± 0.06	6.92 ± 0.06	0.10 ± 0.05
s3	2.14 ± 0.06	8.80 ± 0.06	0.38 ± 0.05

(a) Gloss intensity was obtained by integrating the scattered light intensity in the scattered profile in *Figure* 9a within the angular range 45° ± 0.9°. This value is similar to the specular gloss measurements.
The error bars represent an estimated standard deviation (k=1).

SUMMARY

Characterization of scratch response including deformation pattern, scratch width/depth, and the onset from elastic to plastic deformation was determined for the PMMA and PP commercial samples using a proposed measurement protocol (PICSTP). The deformation patterns observed in each material were quite different. The critical force for plastic deformation was determined to depend on both the scratch velocity and the tip shape. Optical scattering experiments carried out on scratches above and below the critical force were able to distinguish the severity of the scratch. Scattering profiles of scratches at various scattering configurations provide a quantitative way to evaluate the scratch resistance and are the subject of continued research.

ACKNOWLEDGMENTS

Reference

(1) Betz, P. and Bartelt, A., "Scratch Resistant Clear Coats: Development of New Testing Methods for Improved Coatings," *Prog. Org. Coat.*, 22, 27-37 (1993).

(2) Shen, W., Ji, C., Jones, F., Everson, M.P., and Ryntz, R.A., "Measurement by Scanning Force Microscopy of the Scratch and Mar Resistance of Surface Coatings," *Surf. Coat. International*, 6, 253-256 (1996).

(3) Ryntz, R.A., Abell, B.D., Pollano, G.M., Nguyen, L.H., and Shen, W.C., "Scratch Resistance Behavior of Model Coating Systems," JOURNAL OF COATINGS TECHNOLOGY, 72, No. 904, 47-53 (2000).

(4) Lin, L., Blackman, G.S., and Matheson, R.R., "Quantitative Characterization of Scratch and Mar Behavior of Polymer Coatings," *Mater. Sci. Eng.*, A 317, 163-170 (2001).

(5) Jardret, V., Lucas, B.N., Oliver, W., and Ramamurthy, A.C., "Scratch Durability of Automotive Clear Coatings: A Quantitative, Reliable and Robust Methodology," JOURNAL OF COATINGS TECHNOLOGY, 72, No. 907, 79 (2000).

(6) Ryntz, R.A. and Britz, D., "Scratch Resistance Behavior of Automotive Plastic Coatings," JOURNAL OF COATINGS TECHNOLOGY, 74, No. 925, 77 (2002).

(7) Krupicka, A., Johansson, M., Wanstrand, O., and Hult, A., "Mechanical Response of Ductile Polymer Coatings to Contact and Tensile Deformation," *Prog. Org. Coat.*, 48, 1-13 (2003).

(8) Courter, J.L. and Kamenetzky, E.A., "Micro- and Nano-Indentation and Scratching for Evaluating the Mar Resistance of Automotive Clearcoats," *Eur. Coat. J.*, 7, 24-38 (1999).

(9) Courter, J.L., "Mar Resistance of Automotive Clearcoats: 1. Relationship to Coating Mechanical Properties," JOURNAL OF COATINGS TECHNOLOGY, 69, No. 866, 57 (1997).

(10) Pangarajan, P., Sinha, M., Watkins, V., Harding, K., and Sparks, J., "Scratch Visibility of Polymers Measured using Optical Imaging," *Mater. Eng. Sci.*, 43 (3), 749-758 (2003).

(11) Fernholz, K., Sinha, M., Gardner, M., and Watkins, V., "Scratch Visibility: Application of GE's Visual Quality Method at Ford," *Proc. 7th International Coatings for Plastics Symposium*, Troy, MI, June 7-9, 2004.

(12) NIST-Industry Polymer Interphase Consortium (PIC)—more details: visit the PIC consortium website at slp.nist.gov.

(13) VanLandingham, M.R., Chang, N.K., Wu, T.Y., Sung, L., Jardret, V.D., and Chang, S.H., "Measurement Approaches to Develop a Fundamental Understanding of Scratch and Mar Resistance," JCT RESEARCH, 1, No. 4, p 257-266 (2004).

(14) Corle, T.R. and Kino, G.S., "Confocal Scanning Optical Microscopy and Related Imaging Systems," Academic Press, 37-39, 1996.

(15) Sung, L., Jasmin, J., Gu, X., Nguyen, T., and Martin, J.W., "Use of Laser Scanning Confocal Microscopy for Characterizing Changes in Film Thickness and Local Surface Morphology of UV-Exposed Polymer Coatings," JCT RESEARCH, 1, No. 4, p. 267 (2004).

(16) Sung, L., Garver, J., Embree, E., Dickens, B., and Martin, J.W., "A Novel Light Scattering Instrument for Characterizing Polymer Coatings and Plastics," in press, *Rev. Sci. Instrum.* (2005).

(17) Briscoe, B.J., Pelillo, E., and Sinha, S.K., "Scratch Hardness and Deformation Maps for Polycarbonate and Polyethylene," *Polym. Eng. Sci.*, 36 (24), 2996-3005 (1996).

(18) Jardret, V. and Morel, P., "Viscoelastic Effects on the Scratch Resistance of Polymers: Relationship Between Mechanical Properties and Scratch Properties at Various Temperatures," *Prog. Org. Coat.*, 48, 322-331 (2003).

(19) VanLandingham, M.R., "A Review of Instrumented Indentation," *J. Res. NIST*, 108 (4), 249-265 (2003).

(20) VanLandingham, M.R., Camara, R., and Villarrubia, J.S., "Measuring Tip Shape for Instrumented Indentation Using Atomic Force Microscopy," in press, *J. Mater. Res.* (2005).